

See discussions, stats, and author profiles for this publication at: <https://www.researchgate.net/publication/224079961>

True Inline Cross-Coupled Coaxial Cavity Filters

Article in *IEEE Transactions on Microwave Theory and Techniques* · January 2010

DOI: 10.1109/TMTT.2009.2034221 · Source: IEEE Xplore

CITATIONS

45

READS

843

2 authors:



Ying Wang

Ontario Tech University

61 PUBLICATIONS 689 CITATIONS

SEE PROFILE



Ming Yu

The Chinese University of Hong Kong

136 PUBLICATIONS 1,674 CITATIONS

SEE PROFILE

Some of the authors of this publication are also working on these related projects:



A Modular and Scalable Architecture for Millimeter-Wave Beam-forming Antenna Systems [View project](#)

True Inline Cross-Coupled Coaxial Cavity Filters

Ying Wang, *Member, IEEE*, and Ming Yu, *Fellow, IEEE*

Abstract—In this paper, a novel true inline configuration for cross-coupled coaxial cavity filters is presented, which is characterized by a simple and compact structure, improved performance, and good tunability. Instead of using folded structures, dedicated coupling probes, or extra cavities, as required by conventional techniques, cross coupling is realized by changing the orientation of selected resonators. Sequential coupling between adjacent resonators and cross coupling between nonadjacent resonators are effectively controlled by introducing small metal plates at different locations. A six-pole bandpass filter with two transmission zeros was built and tested. The measurement and simulation results agree very well, demonstrating feasibility of the inline filter configuration. It enables compact design with improved resonator Q compared to conventional combline filters. Furthermore, cross coupling can be readily adjusted using tuning elements.

Index Terms—Coaxial cavity filters, combline filters, cross coupling, inline filters, microwave filters.

I. INTRODUCTION

IN microwave bandpass filter design, transmission zeros on one or both sides of the passband are frequently required in order to meet increasingly stringent rejection requirements. Transmission zeros can be readily realized using cross coupling [1], [2]. Folded structures are usually necessary for convenient realization of coupling between nonadjacent resonators. However, they are not suitable when there is structural constraint of inline configuration. In addition, input and output connectors are sometimes required to be placed on opposite sides of the two end resonators. For waveguide filters, inline configuration can be realized using cross coupling between multimode cavities [3] or extracted pole cavities [4]. Other techniques include using higher order modes for the implementation of the two signal paths required for the generation of a transmission zero [5], application of nonresonating nodes [6], and use of rectangular ridges arbitrarily oriented within a waveguide [7]. Most of the techniques based on waveguide technologies cannot be directly applied for coaxial cavity filters, which is the focus of this paper. For coaxial cavity filters, the techniques that are suitable for realizing transmission zeros for inline configuration include the extracted pole technique [4] and the application of nonresonating nodes [8]. However, both techniques require additional

resonating or nonresonating structures and may lead to spurious peaks at out-of-band frequencies [9]. Furthermore, for an inline implementation, it is necessary to couple the input and output to the second and the second to last resonators. Additional wirings are needed in order to move connectors to the two ends of the filter housing.

Another well-known solution for combline filters is to use a coupling probe embedded in the housing of the filter. Fig. 1(a) demonstrates the coupling and routing schematic of an example six-pole filter with one transmission zero. In Fig. 1(b), the cross coupling between resonator 1 and 3 is realized by a probe across three resonators. However, such a long probe generates unwanted resonances. Fig. 1(c) shows the full electromagnetic (EM) simulation results of the six-pole filter example centered at 1.54 GHz using HFSS [10]. Besides generating a transmission zero above the filter passband, the coupling probe resonates and generates a spike in the lower stop band as shown in Fig. 1(c). Another disadvantage for such an implementation is that tuning of the cross coupling becomes difficult.

In this paper, we present a true inline configuration for coaxial cavity filters characterized by simple and compact structure, improved performance, and good tunability (patent pending). Instead of using folded structures, dedicated coupling probes, or extra cavities, as required by conventional techniques, cross coupling between nonadjacent resonators is realized by changing the orientation of selected resonators. Sequential coupling between adjacent resonators is effectively controlled by introducing small metal plates at different locations. Input and output connectors can be conveniently positioned at the two ends of the filter housing. The proposed filter configuration enables compact design with an improvement in the resonator Q factors compared to conventional combline filters. Furthermore, filter tunability is improved due to the fact that cross coupling can be readily adjusted using tuning elements. A six-pole bandpass filter with two transmission zeros using the inline configuration was manufactured, tuned, and tested. The measurement results are presented and practical issues in the design and tuning of the filter are discussed.

II. PROPOSED INLINE CONFIGURATION

A. Filter Configuration

For combline filters, the coupling between nonadjacent resonators is minimized in an inline configuration [11]. Coupling probes are therefore usually needed in order to introduce cross coupling. In the inline configuration proposed herein, cross coupling is realized by changing the orientation of selected resonators. Fig. 2 utilizes a three-pole coaxial cavity filter example for demonstration. Unlike combline filters, the second resonator is rotated by 90° . As a result, besides sequential coupling between resonators 1 and 2 and between resonators 2 and 3, there

Manuscript received May 04, 2009; revised July 24, 2009. First published November 13, 2009; current version published December 09, 2009. This work was supported in part by the Natural Sciences and Engineering Research Council of Canada and by COM DEV, Ltd..

Y. Wang is with the Faculty of Engineering and Applied Sciences, University of Ontario Institute of Technology, Oshawa, ON L1H 7K4 Canada (e-mail: ying.wang@uoit.ca).

M. Yu is with COM DEV, Ltd., Cambridge, ON N1R 7H6 Canada (e-mail: ming.yu@ieee.org).

Color versions of one or more of the figures in this paper are available online at <http://ieeexplore.ieee.org>.

Digital Object Identifier 10.1109/TMTT.2009.2034221

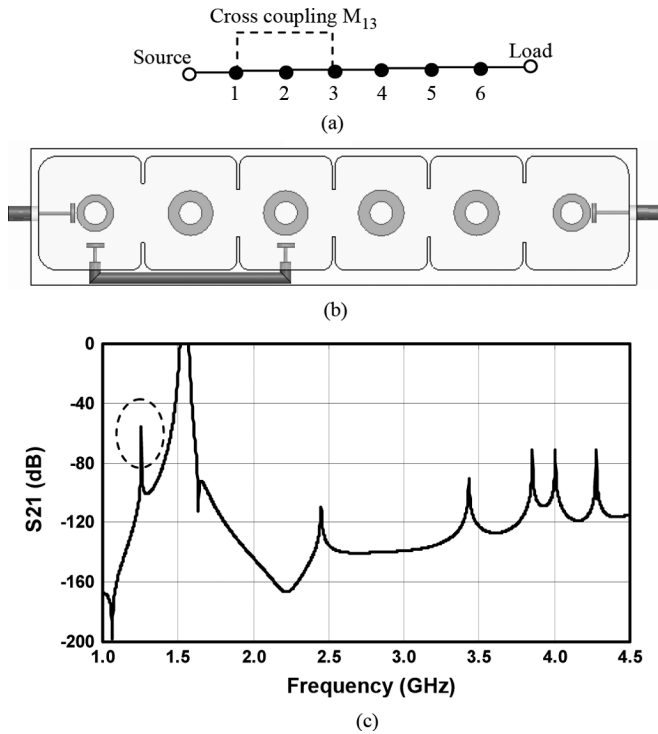


Fig. 1. (a) Coupling and routing schematic of an example of a six-pole filter with one transmission zero. (b) Realization of transmission zero using coupling probe embedded in the housing of the filter. (c) EM simulation of the filter transfer function shows that besides generating a transmission zero above the filter passband, the coupling probe resonates and generates a spike.

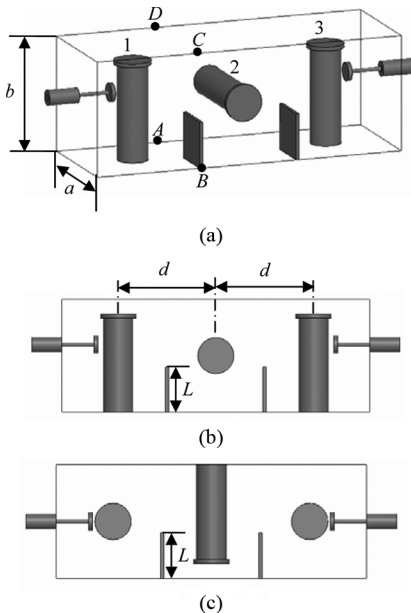


Fig. 2. (a) Perspective view, (b) side view, and (c) top view of the inline configuration.

is direct coupling between resonators 1 and 3, which creates a trisection and consequently a transmission zero.

Intuitively, changing the distances between resonators and iris sizes would cause both sequential-coupling and cross-coupling values to change at the same time, since both types of coupling are strongly affected by these parameters. The main difficulty is

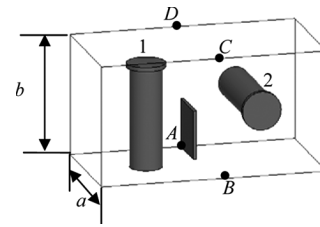


Fig. 3. Two resonator structure for calculation of sequential coupling.

effectively controlling sequential coupling and cross coupling separately. Since fields in cavity 2 are perpendicular to those in cavities 1 and 3, a solution to the problem is greatly facilitated by the introduction of small rectangular metal plates in the corner of the cavity between coaxial resonators. Two metal plates, each of size $L \times L$, are shown in Fig. 2. By proper arrangement of locations and sizes of the plates and distances between resonators, the desired coupling coefficients can be realized as detailed below.

Note that the middle resonator may be rotated to other angles to control coupling values. However, practical implementation will become difficult.

B. Control of Sequential and Cross Coupling

Without the small plates in between, the coupling between adjacent resonators is dominantly magnetic coupling, and the total coupling is the magnetic coupling less the electric coupling, which is very similar to the combline configuration [2], [12]. Rotation of one of the resonators by 90° makes the inter-resonator coupling less effective compared to a combline configuration. Resonators can be placed closer together to increase coupling, which results in a more compact design. More importantly, small plates are introduced to allow a wide range of adjustment of coupling between adjacent resonators.

In order to demonstrate how the coupling coefficient is affected by locations and sizes of the coupling plate and the resonator distances, the structure shown in Fig. 3 with only two resonators is used. As an example, the cavity width a and height b are assumed to both be 1.5 in. The resonators have 0.4-in diameter and 1.3-in height. The distance between the centers of the resonators to each of the three closest side walls along the orientation of the resonator is fixed, which is always half of the cavity width. For example, the distance between the center of resonator 1 to each of the three vertical side walls is 0.75 in. The thickness of the coupling plate is 0.04 in.

Due to the fact that resonators 1 and 2 are not identical, the coupling coefficient cannot be calculated by placing a perfect electric conductor wall and a perfect magnetic conductor wall between resonators [13]–[15]. However, when the two resonators have the same resonance frequencies, the following equation is used to calculate the coupling coefficient k :

$$|k| = \left| \frac{f_1^2 - f_2^2}{f_1^2 + f_2^2} \right| \quad (1)$$

where f_1 and f_2 are the two eigenmodes of the structure in Fig. 3. They can be calculated using the eigenmode solver of an EM simulator [10].

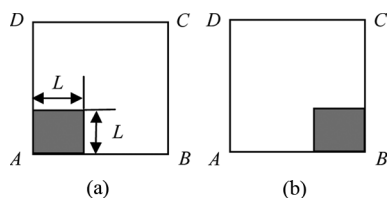


Fig. 4. Side view of the small plates between resonators with different locations (a) at corner A and (b) at corner B .

When a small plate is introduced at corner A , as shown in Figs. 3 and 4(a), resonators 1 and 2 have exactly the same cavity dimensions since the cavity width a and height b are the same and the plate has a squared shape as shown in Fig. 4, except for a 90° rotation of the center posts. Therefore, the condition that both resonators have the same resonance frequencies can be easily met. However, when the plate is introduced at corner B , as shown in Figs. 2 and 4(b), the plate is close to the bottom of resonator 1 and the top of resonator 2. When the two resonators have the exact same dimensions, they do not have the same resonance frequencies. To obtain a good approximation of the coupling value, each resonator is first simulated individually with the other resonator completely detuned. Detuning can be done by short-circuiting one of the resonators, e.g., resonator 2. The resonance frequency f_1 of resonator 1 is calculated. The resonance frequency f_2 of resonator 2 is then calculated by detuning resonator 1. If f_1 and f_2 are different, resonator dimensions are adjusted and resonance frequencies are recalculated until they are the same. This extra step is only to make sure that each resonator by itself, without the presence of the other, resonates at the same frequency. The coupling coefficient k can then be calculated by coupling the two resonators as shown in Fig. 3 and using (1). As will be proven by simulation and measurement results, good initial values can be obtained following these steps.

Fig. 5 shows simulated coupling coefficients as locations and sizes of the plate and the resonator distances vary. Fig. 5(a) demonstrates that when the plate is at corner A , the coupling coefficient reduces as the plate becomes larger. The reason is that such a small plate reduces magnetic coupling, and thus reduces the total coupling. The coupling coefficient reduces to zero when the size of the plate is about half of the resonator height. The plate size which causes coupling null depends on the dimensions of the resonator. As the electrical length of the resonator gets shorter, coupling null occurs when the plate height is below half of the resonator height. After the plate size increases beyond this point, the coupling changes from magnetic coupling to electric coupling and starts to increase.

On the other hand, if the plate is placed at corner B , the electric coupling is reduced. Therefore, the resulting total coupling increases in Fig. 5(b) as the plate size increases. A plate at corner D has the same effect. When a small plate is placed at corner C , it increases electric coupling and thus reduces the total coupling as shown in Fig. 5(c). After the plate is increased to about half of the resonator height, the coupling changes to electric coupling and starts to increase rapidly. All results show that the coupling reduces as the distance d between resonators increases.

The magnetic cross coupling between resonators 1 and 3 in Fig. 2 gives rise to a positive coupling and therefore generates a

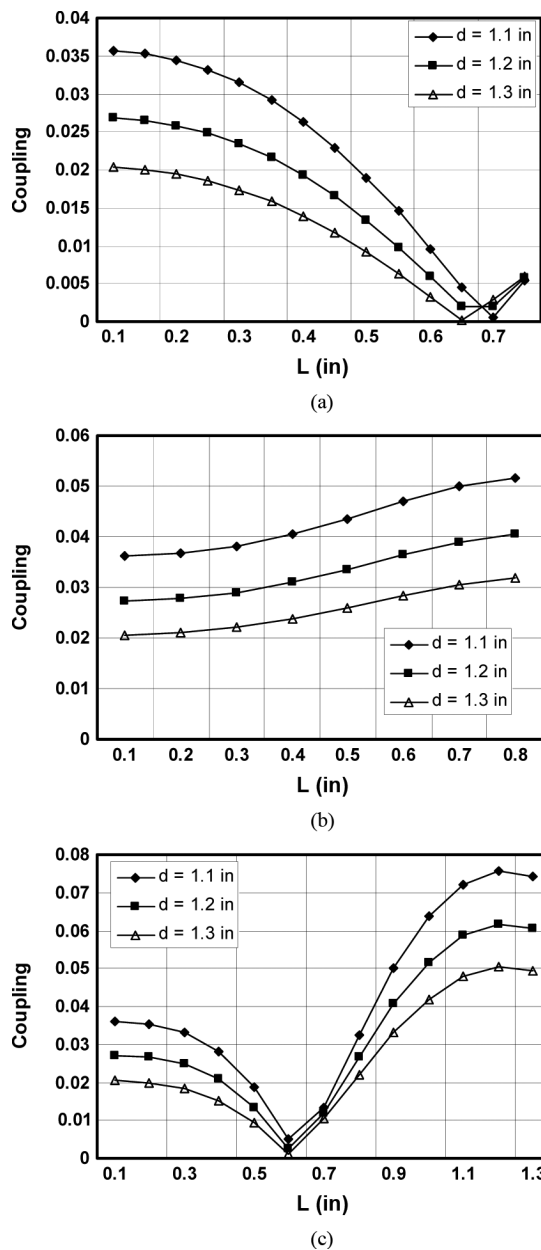


Fig. 5. Sequential-coupling coefficients when the plate is placed at (a) corner A , (b) corner B , and (c) corner C of Fig. 3. The cavity width a and height b are both 1.5 in. All resonators have a 0.4-in diameter and 1.3-in height. Thickness of the plate is 0.04 in.

transmission zero in the upper stop band. A transmission zero in the lower stop band can be created by simply rotating the third resonator 180° vertically as shown in Fig. 6.

A rigorous method of calculating nonadjacent coupling between combline cavities is described in [11]. Here an approximate solution is found by detuning the second resonator in Fig. 2, removing the input/output coupling, and finding the two resonant frequencies using the eigenmode solver of an EM simulator. The coupling coefficient is calculated using (1). Fig. 7 shows that the cross coupling reduces monotonically as the size of the plate increases and as the resonator distance increases when the plate is placed at corner A in Fig. 2. A plate at corner B has the same effect.

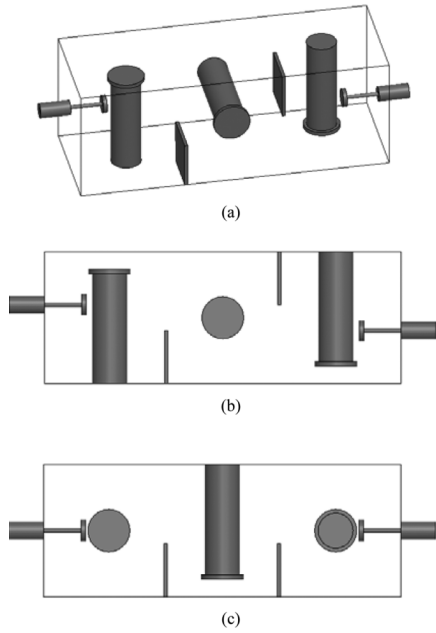


Fig. 6. Filter configuration to realize below passband transmission zero: (a) perspective view, (b) side view, and (c) top view.

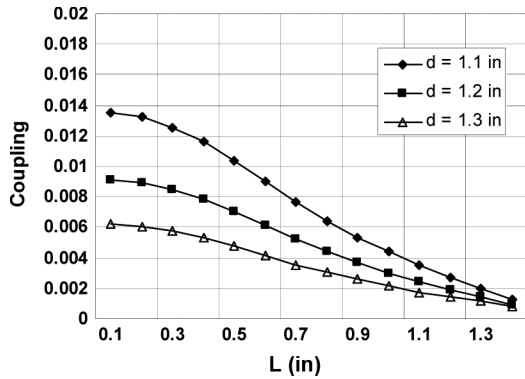


Fig. 7. Cross-coupling coefficients when the plates are placed at corner A in Fig. 2, with input/output coupling removed and resonator 2 detuned. The cavity width a and height b are both 1.5 in. All resonators have a 0.4-in diameter and 1.3-in height. Thickness of each plate is 0.04 in.

It can be seen from Figs. 5(a)–(b) and 7, by simply moving the same sized plate from corner A to corner B, that the sequential coupling can be significantly increased while the cross coupling remains unchanged. A similar effect can be expected when moving a plate from corner C to D, although the cross-coupling values are slightly different from data shown in Fig. 7.

When there is more than one plate between a pair of adjacent resonators, the contribution from each plate may add up or cancel depending on the location of this plate. An example is shown in Fig. 8. The two rectangular plates have the same height L . The plate at corner A has a length of L_A and the plate at corner B has a length of L_B . The sequential coupling between two adjacent resonators and cross coupling between the first and last resonators are calculated as a function of L_B and shown in Fig. 9. The distance between adjacent resonators d is 1.25 in and the height of the plates L is 0.7 in. It is assumed that $L_A + L_B = L$. When L_A reduces to 0 in, the filter in Fig. 8

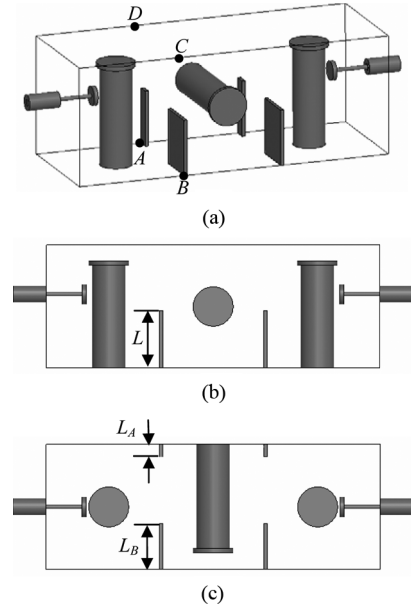


Fig. 8. (a) Perspective view, (b) side view, and (c) top view of the inline configuration with two coupling plates between adjacent resonators.

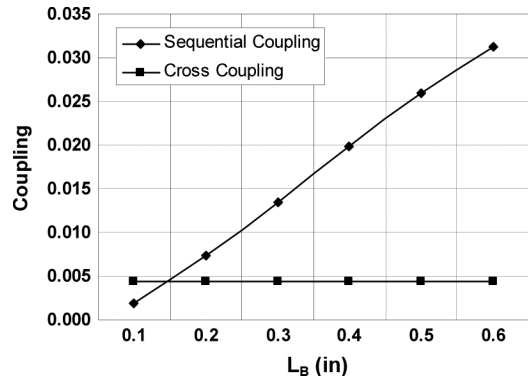


Fig. 9. Sequential- and cross-coupling coefficients of the filter in Fig. 8 as the length of the plate at corner B (L_B) increases. Resonator distance $d = 1.25$ in and height of the plates $L = 0.7$ in. Thickness of each plate is 0.04 in.

has the same configuration as the filter in Fig. 2. The filter in Fig. 8 can therefore be considered as the result of splitting the coupling plate in Fig. 2 into two pieces. As can be seen from Fig. 9, the cross coupling remains unchanged and the sequential coupling increases significantly as the length of coupling plate L_B increases. Therefore, by separating one coupling plate into two pieces, we can individually control sequential coupling and cross coupling.

In addition, the thickness of the coupling plate can be used as another design variable. Fig. 10 shows sequential-coupling and cross-coupling values as the thickness increases when the plate is positioned at corner A. The resonator distance d is 1.3 in, the length and height of the small plate L is 0.3 in, and the rest of the dimensions are as those in Figs. 5 and 7. As can be seen from Fig. 10, changing the thickness of the coupling plate has a similar effect to changing the length and height of the plate. When the plate is at corner A the sequential-coupling coefficient decreases as the thickness of the plate increases. However, it does not have significant impact on cross coupling. Therefore,

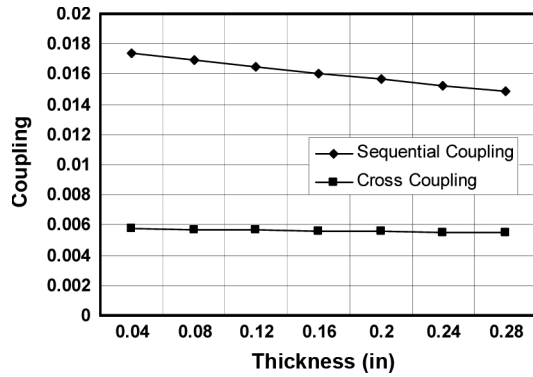


Fig. 10. Sequential- and cross-coupling coefficients versus thickness of the plate when placed at corner *A* in Fig. 2 Resonator distance $d = 1.3$ in and length and height of the small plate $L = 0.3$ in.

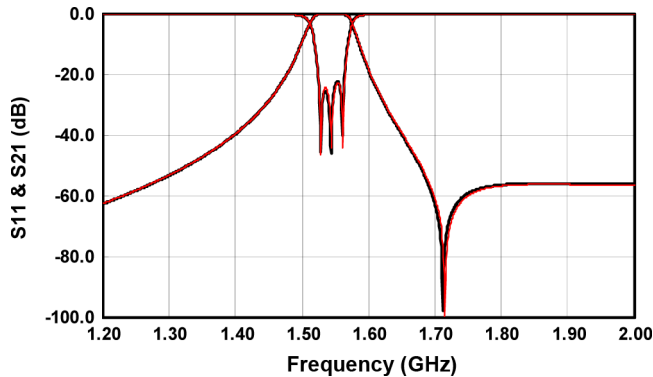


Fig. 11. Comparison of EM simulation results of the filter in Fig. 2 (solid black) and the filter in Fig. 8 (gray or red in an online version), both showing a transmission zero in the upper stop band. The filter in Fig. 2 has one coupling plate between adjacent resonators, while the filter in Fig. 8 has two plates between resonators.

plate thickness can be used for fine adjustment of sequential coupling, once the desired cross coupling is obtained.

In summary, the proposed configuration offers great flexibility for filter design. Besides resonator distance, length, height, and thickness of the coupling plate, location of the plate and the number of coupling plates between adjacent resonators can all be utilized as design parameters. By allowing the size of the plate to vary in all three dimensions or by adding additional plates, the design optimization procedure can be simplified. The designer may also choose to fix certain parameters, e.g., plate thickness, which generally requires iterative design procedure to obtain required coupling values. In the filter examples shown next, the design optimization is carried out through a combination of a full EM model [10] and a circuit model based on a coupling matrix. The circuit model, i.e., coupling matrix, is extracted in every iteration of optimization [16].

Note that the proposed configuration is not limited to coaxial resonators with square cross sections. Rectangular cavities are also applicable. Cavity size can be selected with a conventional tradeoff between Q and filter size. Since horizontally and vertically oriented resonators have similar Q factors, no special consideration is required.

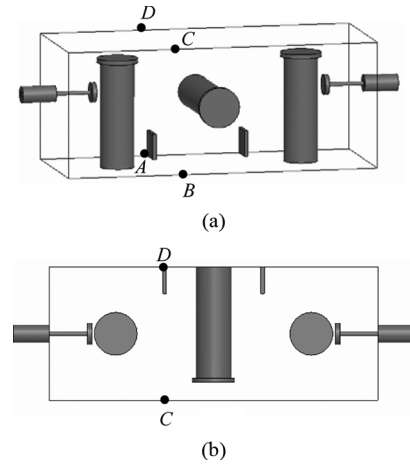


Fig. 12. (a) Perspective view and (b) top view of the inline configuration realizing a higher cross coupling while maintaining the same filter bandwidth.

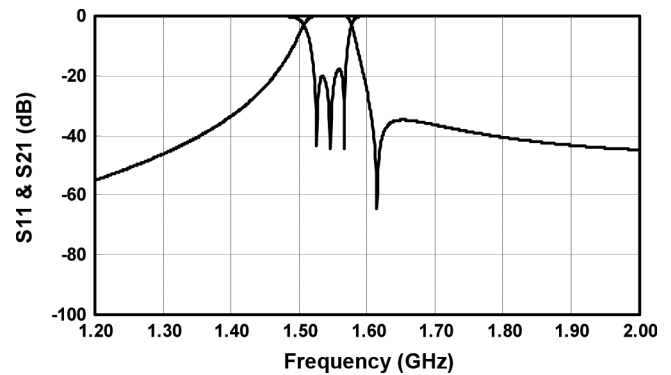


Fig. 13. EM simulation results of the filter in Fig. 12 showing a transmission zero closer to the passband while maintaining the same bandwidth as the previous examples. Resonator distance $d = 1.1$ in and length and height of the small plate $L = 0.3$ in. Thickness of each plate is 0.04 in.

C. Filter Design Examples

In the following, design examples are presented using the proposed inline filter configuration. The cavity width a and height b are assumed to both be 1.5 in. The distance between resonator 1 and the end wall on the input side and the distance between resonator 3 and the end wall on the output side are both 0.75 in. These dimensions remain unchanged for all examples in this section.

In the first example, the filter configuration in Fig. 2 is used to realize a three-pole filter with a transmission zero above its passband. The filter is centered at $f_0 = 1.54$ GHz with the bandwidth $BW = 48.8$ MHz. The normalized coupling matrix is shown in

$$M = \begin{pmatrix} 0.01 & 0.90 & 0.145 \\ 0.90 & -0.15 & 0.90 \\ 0.145 & 0.90 & 0.01 \end{pmatrix} \quad (2)$$

$$R_1 = R_2 = 1.06.$$

The coupling coefficient k can be found using

$$k = M \frac{BW}{f_0}. \quad (3)$$

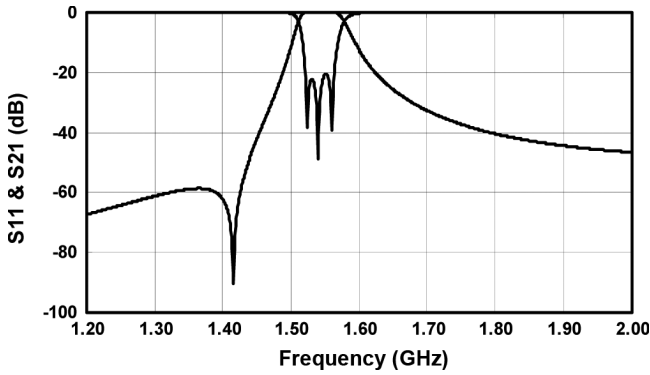


Fig. 14. EM simulation results of the filter in Fig. 6 showing a transmission zero in the lower stop band. Resonator distance $d = 1.27$ in and length and height of the small plate $L = 0.6$ in. Thickness of each plate is 0.04 in.

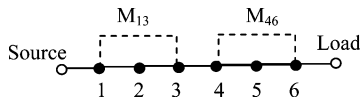


Fig. 15. Coupling and routing schematic of the six-pole filter.

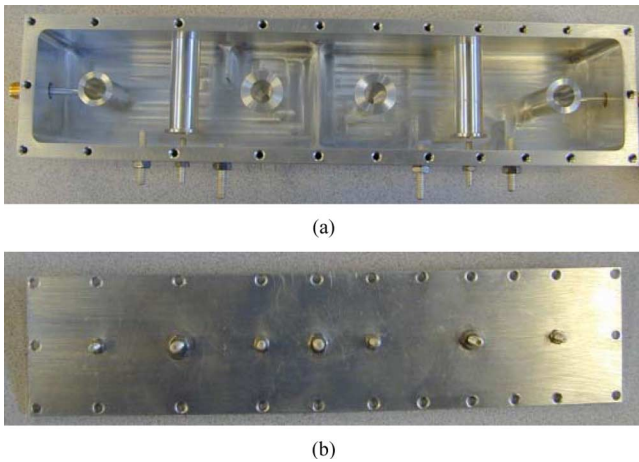


Fig. 16. Pictures of the manufactured inline filter: (a) top view of the filter body with the lid removed and (b) the filter lid.

The corresponding sequential coupling is 0.0285 and the cross coupling is 0.0046. The initial values for resonator distance d and length L of the small plate are estimated using the curves shown in Figs. 5(b) and 7 through interpolation. The filter is then optimized [16] resulting in $d = 1.3$ in and $L = 0.55$ in. Plate thickness is used as a variable during optimization since it allows independent control of sequential and cross couplings. The optimized thickness is 0.08 in. Fig. 11 shows the EM simulation response.

The same coupling values in (2) can be realized using the filter in Fig. 8, in which there are two coupling plates between adjacent resonators. In the first step, the size of the coupling plate and the distance between adjacent resonators are selected to realize the required cross-coupling value as if a single coupling plate were to be used. From Fig. 7, d is selected to be 1.25 in and L is 0.7 in. As shown in Fig. 9, for the selected dimensions, the realizable sequential coupling has a wide range. The desired coupling value is obtained when the length of the plates at corner

TABLE I
DIMENSIONS OF MANUFACTURED INLINE FILTER

Parameter	Value
Distance between resonator 1 and end wall (source side)	0.75 in
Distance between resonators 1 and 2	1.12 in
Distance between resonators 2 and 3	1.1 in
Distance between resonators 3 and 4	1.5 in
Distance between resonators 4 and 5	1.35 in
Distance between resonators 5 and 6	1.2 in
Distance between resonator 6 and end wall (load side)	0.75 in
Length and height of plate between resonators 2 and 3	0.48 in
Length and height of plate between resonators 4 and 5	0.38 in
Length and height of plate between resonators 5 and 6	0.475 in
Height of half wall between resonators 3 and 4	0.815 in

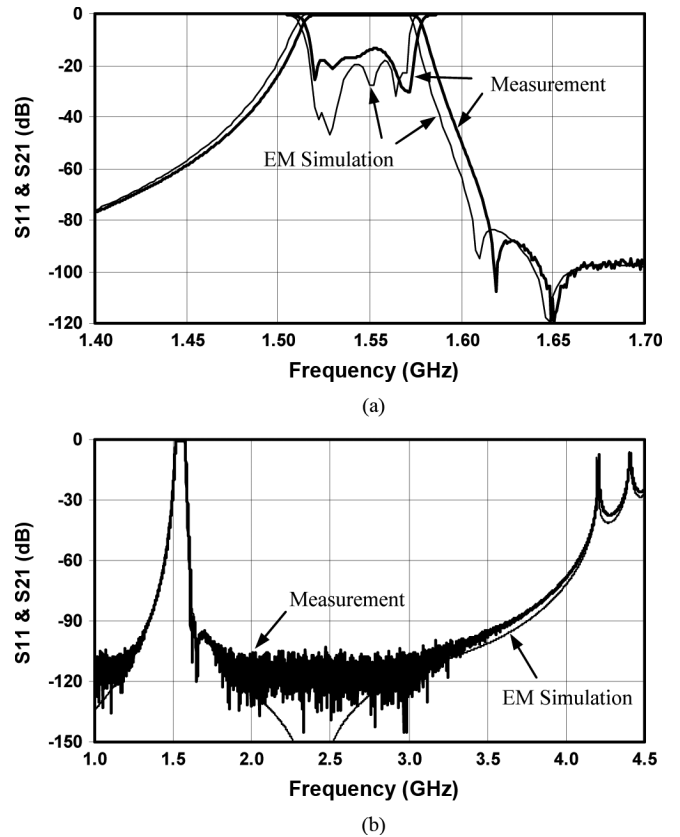


Fig. 17. Comparison of initial measurement (bold lines) with EM simulation results: (a) near-band responses of return loss and insertion loss and (b) wide-band responses of insertion loss. Both measurement and simulation are without tuning elements.

$A (L_A)$ is 0.15 in and the length of the plates at corner $B (L_B)$ is 0.55 in. The EM simulation results are shown in Fig. 11, which show the same response as the previous example. Plate thickness is kept unchanged in this case at 0.04 in.

The next filter example has the same bandwidth. The cross coupling is increased to $k = 0.011$ or $M = 0.35$. The resonators are moved closer together to increase cross coupling, which increases the sequential coupling at the same time. The small plates are changed to corner A as shown in Fig. 12 to

reduce the sequential coupling. The optimized simulation response is shown in Fig. 13, where $d = 1.1$ in and $L = 0.3$ in. The thickness of each coupling plate is 0.04 in. The same bandwidth as in the previous examples is realized using a different resonator distance, size, and location of the plate, resulting in a different out-of-band rejection level.

In the last example, the filter configuration in Fig. 6 is used to realize a three-pole filter with a transmission zero below its passband. The resonators are brought slightly closer together than in the first example to realize the same bandwidth as previous examples. Fig. 14 shows the optimized response from EM simulation, in which resonator distance $d = 1.27$ in, length, and height of the small plate $L = 0.6$ in and the thickness of each coupling plate is 0.04 in.

III. EXPERIMENTAL RESULTS

A six-pole bandpass filter with a center frequency of 1.54 GHz and bandwidth of 48.8 MHz was designed, built, and tested. Its coupling matrix is given by

$$M = \begin{pmatrix} -0.017 & 0.991 & 0.280 & 0 & 0 & 0 \\ 0.991 & -0.361 & 0.665 & 0 & 0 & 0 \\ 0.280 & 0.665 & 0.087 & 0.663 & 0 & 0 \\ 0 & 0 & 0.663 & 0.070 & 0.681 & 0.175 \\ 0 & 0 & 0 & 0.681 & -0.214 & 1.001 \\ 0 & 0 & 0 & 0.175 & 1.001 & 0.051 \end{pmatrix}$$

$$R_1 = R_2 = 1.335.$$

Fig. 15 shows the coupling and routing schematic.

After initial physical dimensions were obtained using the techniques described above, the filter was optimized using the method in [16] with the dimensions shown in Table I. The cavity width and height were both 1.5 in and the overall length was 7.77 in. The resonators each had a 0.4-in diameter and a 1.3-in height. Thickness of each coupling plate was 0.04 in. Pictures of the manufactured inline filter are shown in Fig. 16, with input and output connectors located on the opposite sides of the two end resonators. The initial measurement response without any tuning is shown in Fig. 17. A good agreement can be observed between the EM simulation and measurement results. The wideband results in Fig. 17(b) show much improved out-of-band rejection compared to Fig. 1(c) where a coupling probe is used to realize cross coupling.

Next, tuning elements are introduced to explore tunability of the filter. As shown in Fig. 16(b), tuning screws are placed on the lid between resonators 1 and 3, and between resonators 4 and 6 to facilitate tuning of cross coupling, which also has relatively small effects on sequential coupling. Tuning screws for adjusting sequential coupling are placed on the side wall between adjacent resonators, which provide good tuning range and have minimum impact on cross coupling. Thus, all coupling values can be effectively adjusted. Experimentation with tuning of the cross coupling shows that the inner notch can be readily adjusted by 4 dB. The measured response after tuning is shown in Fig. 18 together with EM simulation results with tuning elements. Note that the center frequency has shifted downward since the frequency tuning screw above each resonator can only reduce the resonance frequency.

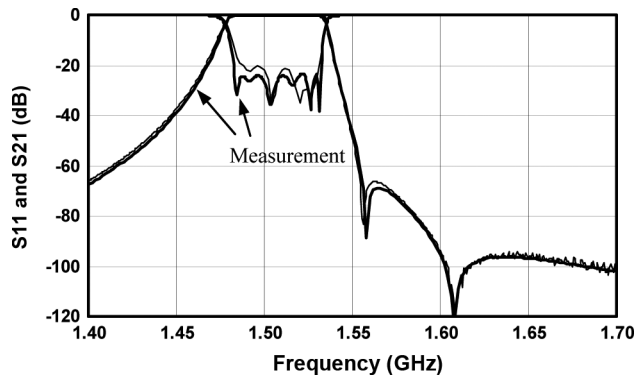
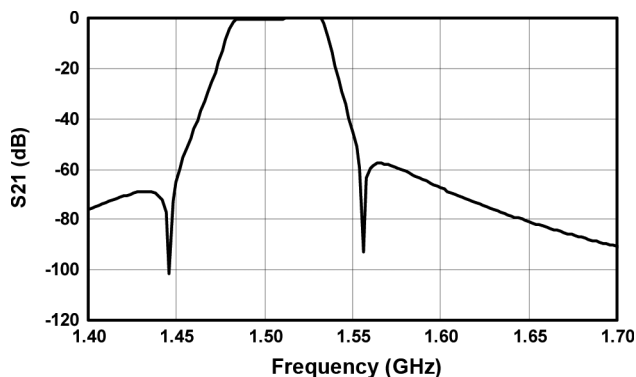
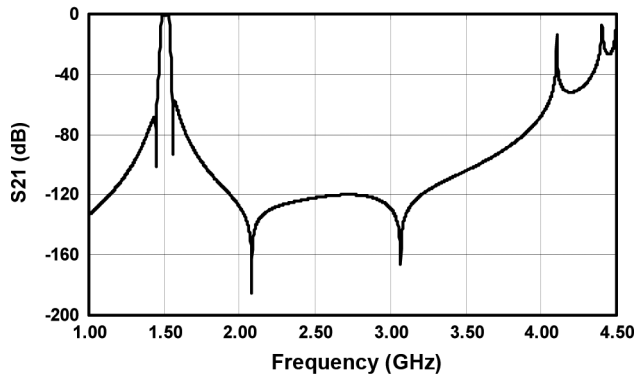


Fig. 18. Comparison of measurement (bold lines) with EM simulation results. Both measurement and simulation are with tuning elements.



(a)



(b)

Fig. 19. EM simulation results of a six-pole bandpass filter with one transmission zero in the upper stop band and one in the lower stop band: (a) near-band response and (b) wideband response of insertion loss.

The measured resonator Q is 4400, which is slightly lower than the simulated Q of 4900 considering nonideal factors such as surface roughness. EM simulation of the conventional combline filter shown in Fig. 1(b) with the same filter size shows a resonator Q of 4500. The results demonstrate that by removing most of the vertical irises needed in the combline filter the cavity size is in effect increased and thereby results in an 8% improvement in the resonator Q factor.

Another simulation is performed to demonstrate design flexibility by simply rotating the last resonator, resonator 6, by 180° vertically and shifting the small plate between resonators 5 and

6 from the current location, i.e., corner B , to corner A to maintain the coupling coefficient. As a result, one of the transmission zeros is moved to the lower stop band as shown in the near-band EM simulation results in Fig. 19(a). The wideband EM simulation result in Fig. 19(b), similar to Fig. 17(b), shows improved out-of-band rejection without any spurious resonance close to filter passband.

IV. CONCLUSION

An inline configuration for coaxial cavity filters which allows coupling between nonadjacent resonators without additional structural complexities is presented in this paper. Cross coupling is realized by changing the orientation of selected resonators. Small metal plates are introduced between resonators to effectively control sequential coupling between adjacent resonators and cross coupling between nonadjacent resonators. The available design parameters include resonator distance, length, height, and thickness of the coupling plate, location of the plate, and the number of coupling plates between adjacent resonators, which offer great flexibility for filter design. The novel filter configuration enables true inline implementation. It allows a more compact design with improvement in the resonator Q compared to conventional combline design. Furthermore, cross coupling can be adjusted using tuning elements. A six-pole bandpass filter with two transmission zeros was built and tested. The measurement and simulation results agree very well demonstrating feasibility of the inline filter configuration.

ACKNOWLEDGMENT

The authors would like to thank V. Dokas of COM DEV, Ltd., Cambridge, ON, Canada, for his help on filter tuning and testing. They would also like to thank the reviewers for constructive comments, which inspired some of the ideas presented herein.

REFERENCES

- [1] R. J. Cameron, "General coupling matrix synthesis methods for Chebyshev filtering functions," *IEEE Trans. Microw. Theory Tech.*, vol. 47, no. 4, pp. 433–442, Apr. 1999.
- [2] J. B. Thomas, "Cross-coupling in coaxial cavity filters—A tutorial overview," *IEEE Trans. Microw. Theory Tech.*, vol. 51, no. 4, pp. 1368–1376, Apr. 2003.
- [3] A. E. Atia and A. E. Williams, "Narrow-bandpass waveguide filters," *IEEE Trans. Microw. Theory Tech.*, vol. MTT-20, no. 4, pp. 258–265, Apr. 1972.
- [4] J. R. Rhodes and R. J. Cameron, "General extracted pole synthesis technique with application to low-loss TE₀₁₁-mode filters," *IEEE Trans. Microw. Theory Tech.*, vol. MTT-28, no. 9, pp. 1018–1028, Sep. 1980.
- [5] M. Guglielmi, F. Montauti, L. Pellegrini, and P. Arcionj, "Implementing transmission zeros in inductive-window bandpass filters," *IEEE Trans. Microw. Theory Tech.*, vol. 43, no. 8, pp. 1911–1915, Aug. 1995.
- [6] S. Amari, U. Rosenberg, and J. Bornemann, "Singlets, cascaded singlets and the nonresonating node model for modular design of advanced microwave filters," *IEEE Microw. Wireless Compon. Lett.*, vol. 14, no. 5, pp. 237–239, May 2004.
- [7] S. Bastioli, L. Marcaccioli, and R. Sorrentino, "Waveguide pseudoelliptic filters using slant and transverse rectangular ridge resonators," *IEEE Trans. Microw. Theory Tech.*, vol. 56, no. 12, pp. 3129–3136, Dec. 2008.
- [8] S. Amari and G. Macchiarella, "Synthesis of inline filters with arbitrarily placed attenuation poles by using nonresonating nodes," *IEEE Trans. Microw. Theory Tech.*, vol. 53, no. 10, pp. 3075–3081, Oct. 2005.

- [9] S. Cogollos, R. J. Cameron, R. R. Mansour, M. Yu, and V. E. Boria, "Synthesis and design procedure for high performance waveguide filters based on nonresonating nodes," in *IEEE MTT-S Int. Microw. Symp. Dig.*, Honolulu, HI, Jun. 2007, pp. 1297–1300.
- [10] *Ansoft HFSS*, Ver. 11, Ansoft Corporation, Pittsburgh, PA, 2007.
- [11] M. E. Sabbagh, K. A. Zaki, H. Yao, and M. Yu, "Full-wave analysis of coupling between combline resonators and its application to combline filters with canonical configurations," *IEEE Trans. Microw. Theory Tech.*, vol. 49, no. 12, pp. 2384–2393, Dec. 2001.
- [12] R. W. Rhea, *HF Filter Design and Computer Simulation*. Atlanta, GA, Noble: , 1994.
- [13] R. J. Cameron, C. M. Kudsia, and R. R. Mansour, *Microwave Filters for Communication Systems: Fundamentals, Design and Applications*. New York: Wiley, 2007.
- [14] H.-W. Yao, K. A. Zaki, A. E. Atia, and R. Hershtig, "Full-wave modeling of conducting posts in rectangular waveguides and its applications to slot coupled combline filters," *IEEE Trans. Microw. Theory Tech.*, vol. 43, no. 12, pp. 2824–2830, Dec. 1995.
- [15] C. Wang, H. Yao, K. A. Zaki, and R. R. Mansour, "Mixed modes cylindrical planar dielectric resonator filters with rectangular enclosure," *IEEE Trans. Microw. Theory Tech.*, vol. 43, no. 12, pp. 2817–2823, Dec. 1995.
- [16] M. A. Ismail, D. Smith, A. Panariello, Y. Wang, and M. Yu, "Em-based design of large-scale dielectric-resonator filters and multiplexers by space mapping," *IEEE Trans. Microw. Theory Tech.*, vol. 52, no. 1, pt. 2, pp. 386–392, Jan. 2004.



Ying Wang (M'05) received the B.Eng. and M.S. degrees in electronic engineering from Nanjing University of Science and Technology, Nanjing, China, in 1993 and 1996, respectively, and the Ph.D. degree in electrical engineering from University of Waterloo, Waterloo, ON, Canada, in 2000.

From 2000 to 2007, she was with COM DEV, Cambridge, ON, Canada, where she was involved in development of computer-aided design (CAD) software for design, simulation, and optimization of microwave circuits for space application. In 2007, she joined the Faculty of Engineering and Applied Science, University of Ontario Institute of Technology, Oshawa, ON, Canada, where she is currently an Assistant Professor. Her research interests include RF/microwave CAD, microwave circuits design, and radio wave propagation modeling.



Ming Yu (S'90–M'93–SM'01–F'09) received the Ph.D. degree in electrical engineering from the University of Victoria, Victoria, BC, Canada, in 1995.

In 1993, while working on his doctoral dissertation part time, he joined COM DEV, Cambridge, ON, Canada, as a Member of Technical Staff. He was involved in designing passive microwave/RF hardware from 300 MHz to 60 GHz for both space- and ground-based applications. He was also a principal developer of a variety of COM DEV's core design and tuning software for microwave filters and multiplexers, including computer-aided tuning software in 1994 and fully automated robotic diplexer tuning system in 1999. His varied experience also includes being the Manager of Filter/Multiplexer Technology (Space Group) and Staff Scientist of Corporate Research and Development (R&D). He is currently the Chief Scientist and Director of R&D. He is responsible for overseeing the development of company R&D Roadmap and next generation products and technologies, including high-frequency and high-power engineering, electromagnetic-based computer-aided design (CAD) and tuning for complex and large problems, novel miniaturization techniques for microwave networks. He is also an Adjunct Professor with the University of Waterloo, ON, Canada. He holds NSERC Discovery Grant from 2004 to 2013. He has authored or coauthored over 90 publications and numerous proprietary reports. He holds eight patents with six more pending.

Dr. Yu is the Vice Chair of MTT-8 and served as Chair of TPC-11. He is a member of the editorial board of many IEEE and IET publications. He was the recipient of the 1995 and 2006 COM DEV Achievement Award for the development of a computer-aided tuning algorithms and systems for microwave filters and multiplexers. He holds the appointment of Distinguished Microwave Lecturer from 2010 to 2012.